ACI MATERIALS JOURNAL TECHNICAL PAPER

Title No. 120-M03

CO_2-Sequestered Cast-in-Place Engineered Cementitious Composites

by Duo Zhang and Victor C. Li

The built environment is facing an increasing challenge of reducing emissions regarding both embodied and operational carbon. As an ultra-durable concrete, engineered cementitious composites (ECC) reduce the need for repair, thus resulting in a prominent reduction of life-cycle footprints. Herein, a new version of low-carbon ECC was developed for cast-in-place applications by sequestering CO_2 through mineralization. Two waste streams were pre-carbonated and incorporated into ECC as fine aggregate and supplementary cementitious material, respectively. At 28 days, the CO_2-sequestered ECC exhibited a compressive strength of 32.2 MPa (4670 psi), tensile strength of 3.5 MPa (508 psi), and strain capacity of 2.9%. Multiple fine cracks were distinctly identified, with a residual crack width of 38 µm (0.0015 in.) and a self-healing behavior comparable to that of conventional ECC. The new ECC sequestered 97.7 kg/m^3 (164.7 lb/yd^3) CO_2 (equivalent to 4.7 wt% of final mixture) and demonstrated a 42% reduction in cradle-to-gate emissions compared to conventional concrete at the same strength level. This study demonstrates the viability of turning waste CO_2 gas into durable construction materials and proposes a potential path towards carbon neutrality.

Keywords: carbon mineralization; carbonation; CO_2 sequestration; durability; engineered cementitious composite (ECC); fly ash; life-cycle assessment; steel slag; sustainability.

INTRODUCTION

The concrete industry is increasingly facing the pressure to reduce emissions. The emissions stem from the expanding demand for both new construction and the frequent renewal of existing infrastructure. As an essential ingredient for making concrete, portland cement (PC) accounts for over 90% of concrete-embodied carbon and is responsible for 5 to 7% of global CO_2 emissions through its production.[1] Complete replacement of PC or removal of its carbon footprint appears to be infeasible in the foreseeable future due to both technical limitation and the established market confidence in PC. As such, sequestering CO_2 becomes a potential route to achieve carbon neutrality for concrete construction.

The quest for sequestering large amounts of CO_2 in concrete received increasing attentions in the past decade, and the relevant technologies span over a wide range of technology readiness levels (TRLs). In the precast industry, carbonation curing has been extensively studied by using CO_2 for curing early-age cement-based products, such as blocks, pavers, and so on.[2] In this process, CO_2 reacts with calcium silicate clinkers and their early hydration products and converts to calcium carbonate as the main carbonate phase.[3] The processing has also been applied to low-hydraulicity binders to activate their cementing ability, such as reactive magnesia[4] and lime.[5] In the cast-in-place market, mixing CO_2 with fresh ready mixed concrete demonstrates a relatively high TRL. Despite a low CO_2 uptake compared to precast carbonation curing, CO_2 mixing improves concrete strength while reducing PC use,[6] and the large market size may leverage a significant sequestration capacity for cast-in-place constructions.

Besides the embodied carbon, CO_2 emissions associated with operation and maintenance (O&M) during the concrete use phase represents an important emission contributor. As a typical brittle material, concrete is weak in tension, and cracks are ubiquitously occurring throughout the lifetime of concrete. Large cracks provide easy pathways for the ingress of harmful species, which accelerate the material deterioration and in turn aggravate further cracking. However, current design and testing for concrete durability are mostly established upon uncracked materials and fail to reflect the impact of cracks in the field. This discrepancy leads to most premature concrete failures, thus incurring the need for repetitive repair and reconstruction. A significant amount of CO_2 emissions are generated during this process and account for a major hurdle for lowering the life-cycle impact associated with the built environment.

Engineered cementitious composite (ECC) is a new class of fiber-reinforced cementitious composites.[7,8] It differs from conventional concrete in its high tensile ductility and strain-hardening characteristics. ECC is designed by tailoring the micromechanics-based parameters associated with fiber, matrix, and fiber-matrix interface such that the material develops multiple fine cracks as opposed to single/few large cracks when overloaded.[9,10] By consistently forming additional cracks, the crack width in ECC can be controlled below 100 µm irrespective of the imposed stress or strain, thus establishing an intrinsic capability of crack width control as a built-in material property.[11] The tight cracks have proven to enhance ECC's durability by keeping a low water permeability,[12] delaying material degradation, and amplifying the self-healing behavior.[13,14] Through the enhanced durability and lowered frequency of repair and reconstruction, ECC demonstrates a substantial reduction in life-cycle impact compared to conventional concrete.[15]

ACI Materials Journal, V. 120, No. 1, January 2023.
MS No. M-2021-458.R1, doi: 10.14359/51737331, received June 24, 2022, and reviewed under Institute publication policies.

ECC may offer an opportunity for turning CO_2 into extremely durable construction materials, hence reducing the embodied and O&M carbon emissions simultaneously. Recent studies demonstrated the feasibility of sequestering CO_2 in precast ECC through carbonation curing and showed promising CO_2 uptake led by its high cementitious content.[16,17] For the cast-in-place application that represents a larger construction market, sequestering CO_2 into ECC would generate a more significant impact. In this study, an experimental investigation is reported on the development of a new CO_2-sequestered ECC by incorporating pre-carbonated industrial by-products as ingredients. Among several alkaline waste streams, steel slag and coal fly ash are chosen for the broad availability. The carbonated fly ash is used as a supplementary cementitious material (SCM), whereas the carbonated steel slag is used as a fine aggregate. The formulated ECC are examined for mechanical and self-healing properties, and an emission reduction analysis is carried out including the A1 through A3 stages (that is, from raw material extraction to manufacturing). The findings of this study demonstrate a new route to convert CO_2 into durable construction materials and would serve as a reference for the field practice of low-carbon concrete.

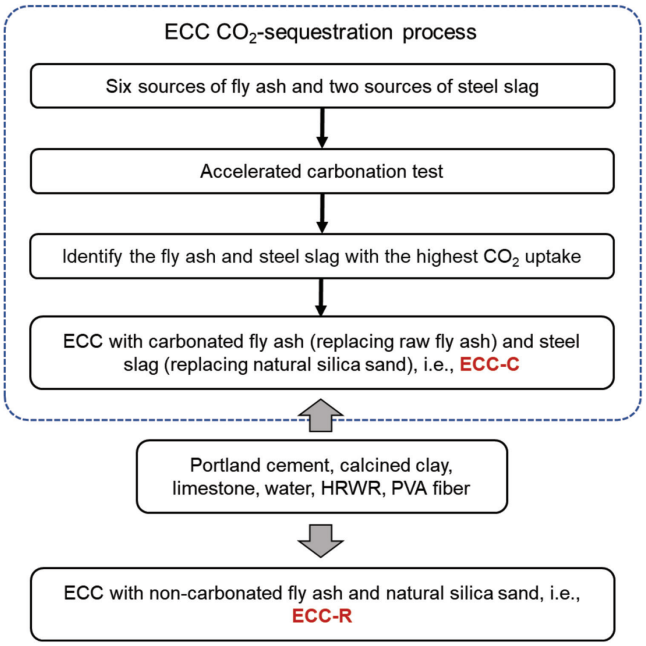

Fig. 1—Overall experimental plan.

RESEARCH SIGNIFICANCE

Concrete sustainability not only means low-carbon construction but also extends to longer service life, less repair, and lower O&M emissions. As a durable material, CO_2-sequestered ECC offers a potential solution to reduce concrete embodied and operational emissions simultaneously. The novel processing and experimental results may facilitate a shift of paradigm in the practice of concrete CO_2 sequestration and would catalyze research and development efforts to synergize emission reduction, waste use, and maintenance-free concrete production. The findings of this study would also support the decision-making processes associated with climate legislation and policy development in the coming wave of infrastructure renewal.

EXPERIMENTAL INVESTIGATION

Figure 1 lays out the overall experimental plan in this study. Six sources of fly ash and two sources of steel slag were examined for CO_2 sequestration. The samples with the highest CO_2 uptake were chosen to formulate ECC. Based on the material characteristics, the carbonated fly ash was used as an SCM to replace the raw fly ash, while the carbonated steel slag was used as a fine aggregate to replace silica sand. The ECC batches made with and without the CO_2-sequestered ingredients are denoted as ECC-C and ECC-R, respectively.

Materials

The raw materials used in this study include ordinary portland cement (OPC, Type I), metakaolin, limestone, fly ash, silica sand, and steel slag. Table 1 lists the chemical compositions of OPC, six sources of fly ash, and two sources of steel slag. Polyvinyl alcohol (PVA) fiber (RECS-15) was used to make ECC, and its technical specifications are listed in Table 2. A polycarboxylate-based high-range water-reducer (HRWR) was added to attain consistent workability. To investigate the source variation in raw materials, fly ash and steel slag were collected from different locations in the Great Lakes region. As listed in Table 1, the fly ash

Table 1—OPC, fly ash, and steel slag chemical compositions, wt%

Oxides	OPC	FA1	FA2	FA3	FA4	FA5	FA6	SS1	SS2
CaO	67.5	27.6	26.5	21.8	28.0	20.2	3.4	40.2	45.2
SiO_2	17.7	32.8	32.9	35.7	33.0	35.5	52.2	33.8	14.6
Al_2O_3	4.2	19.1	19.7	19.5	19.5	21.2	22.2	9.3	3.9
Fe_2O_3	3.7	6.7	6.1	8.3	5.9	10.3	13.5	0.8	27.1
SO_3	3.6	2.1	2.2	3.7	2.8	2.9	2.2	3.7	0.2
MgO	2.0	4.7	4.9	4.3	4.1	3.9	0.9	9.8	3.1
K_2O	0.6	0.7	0.7	0.9	0.6	1.1	2.6	0.7	0.1
TiO_2	0.3	1.3	1.7	1.5	1.6	1.4	1.0	0.7	0.6
MnO	0.1	0.0	0.1	0.0	0.1	0.0	0.0	0.5	3.9
P_2O_5	0.1	1.5	1.5	1.5	1.2	1.1	0.1	0.1	0.8

Table 2—PVA fiber property

Length, mm (in.)	Diameter, μm (×0.001 in.)	Elongation at break, %	Density, kg/m^3 (lb/yd^3)	Young's modulus, GPa (ksi)	Tensile strength, MPa (ksi)
8 (0.315)	39 (1.535)	6	1300 (2191)	42.8 (6208)	1600 (232)

samples have CaO contents varying from 3.4 to 28% and SiO_2 contents from 32.8 to 52.2%. FA1 to FA5 are classified as Class C fly ash, while FA6 is classified as Class F. The two steel slag samples are mainly composed of mineral phases bearing CaO, SiO_2, MgO, and Fe_2O_3. Figure 2 shows the appearance of as-received steel slag samples. Unlike fly ash, steel slag is a relatively coarse material and has a broader range of particle size that is comparable to conventional aggregate. It was thus appropriate to replace the silica sand in conventional ECC as an alternative fine aggregate. Figure 3 compares the particle size distribution between the raw steel slag and silica sand. To maintain consistent particle packing density, steel slag samples were sieved and reproportioned to mimic the particle size distribution of silica sand as shown in Fig. 3(b).

Accelerated carbonation

Mineral carbonation of fly ash and steel slag followed the indirect route and was conducted in an aqueous condition. The raw materials were first mixed with a moderate amount of water to extract CO_2-reactive components. To facilitate a high carbonation efficiency, water is required to provide an aqueous environment while not diluting the Ca and Mg cations significantly. The desirable water content was determined by a set of experimental trial, with the water-to-solid mass ratio varying from 0.05 to 0.30. For each source of fly ash or steel slag, 100 g (0.22 lb) of the sample was tested. After mixing with water, the sample was spread in a thin layer (thickness < 5 mm [0.197 in.]) on an acrylic tray to facilitate CO_2 exposure and placed in a benchtop CO_2 reactor filled with CO_2 gas at a steady pressure of 1.5 bar (21.8 psi) for 1 hour. As a feasibility study, pure CO_2 gas was used for carbonation. The carbonated samples were then measured for the CO_2 uptake using thermogravimetric analysis (TGA). A thermal analyzer was used to heat the samples up to 950°C (1742°F) at a rate of 10°C/min (18°F/min). CO_2 uptake is determined using Eq. (1) and (2)

$$\text{CO}_2\text{ uptake},\% = \frac{(m_{500} - m_{950})/m_{950} - (M_{500} - M_{950})/M_{950}}{1 + \text{LOI}} \times 100\% \quad (1)$$

$$\text{LOI},\% = \frac{M - M_{950}}{M_{950}} \times 100\% \quad (2)$$

where m_{500} is the carbonated sample mass at 500°C (932°F); m_{950} is the carbonated sample mass at 950°C (1742°F); M_{500} is the noncarbonated sample mass at 500°C (932°F); M_{950} is the noncarbonated sample mass at 950°C (1742°F); M is the initial dry mass of the noncarbonated sample; and LOI is loss on ignition of the noncarbonated sample at 950°C (1742°F).

The carbonated steel slag and fly ash were characterized using X-ray powder diffraction (XRD) to identify the phase change and validate the occurrence of mineral carbonation. The steel slag and fly ash samples with the highest

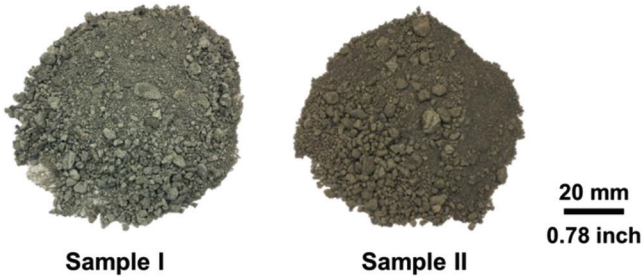

Fig. 2—As-received steel slag appearance.

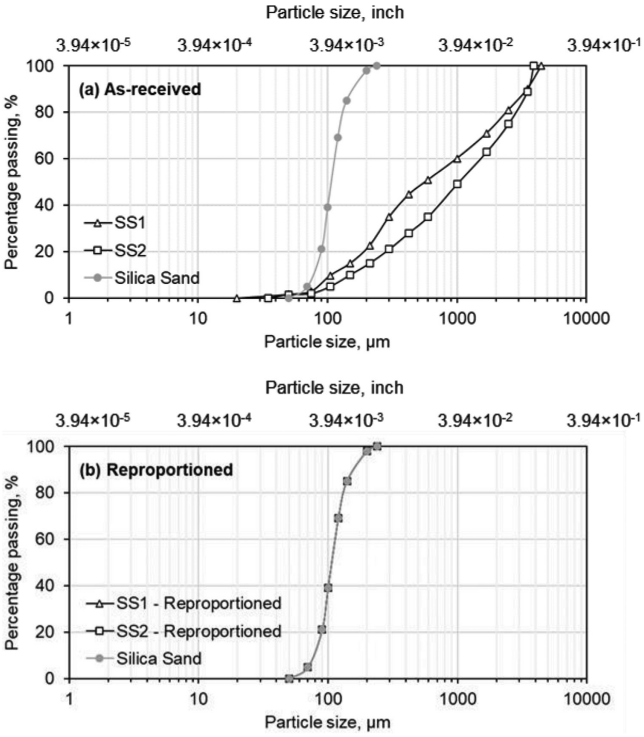

Fig. 3—Particle size distribution of steel slag and silica sand.

CO_2 uptake were chosen to formulate ECC. At the optimal water-to-solid ratio, the samples were carbonated for 2 hours and subsequently dried in a desiccator for 24 hours to attain consistent water contents between ECC-C and ECC-R. This drying procedure can be potentially eliminated in the field by subtracting the free water from the mixing water to minimize the associated energy penalty.

ECC mixing and specimen preparation

Table 3 lists the ECC mixture designs. A low-carbon blend of OPC, metakaolin, and limestone was used in substitution of OPC.[18] The reference ECC (ECC-R) incorporates the noncarbonated fly ash and silica sand, while the CO_2-sequestered ECC (that is, ECC-C) incorporates the carbonated fly ash and carbonated steel slag. As silica sand and steel slag have different specific gravities (2.6 versus 3.3), the two materials were substituted on a volumetric basis. Besides

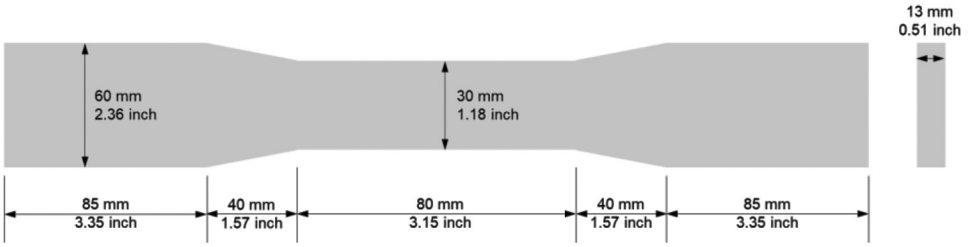

Fig. 4—Dimensions of ECC specimens for uniaxial tension.

Table 3—ECC mixture design (mass ratio)

Composition			ECC-R	ECC-C
Binder	Low-carbon cement	Total	1.0	1.0
		OPC	0.55	0.55
		Metakaolin	0.30	0.30
		Limestone	0.15	0.15
	Fly ash, non-carbonated		2.2	—
	Fly ash, carbonated		—	2.2
Aggregate	Silica sand		1.2	—
	Steel slag, carbonated		—	1.5
Water			0.95	0.95
Water-binder ratio (*w*/*b*)			0.3	0.3
High-range water-reducing admixture (HRWRA)			0.005	0.007
PVA fiber, vol%			2	2

Note: Mixture designs are presented in mass ratio relative to combination of OPC, metakaolin, and limestone (that is, 1.0). ECC-R and ECC-C represent reference group and CO_2-sequestered group, respectively. Silica sand was replaced by carbonated steel slag on volumetric basis. Specific gravity is 2.6 for silica sand and 3.3 for carbonated steel slag.

the solid ingredients, the mixing water content was kept the same for both batches, and the HRWR dosage was adjusted to attain consistent slump flow. PVA fiber was added at a constant 2 vol%.

The mixing process was conducted using a mortar mixer and included the following procedure: 1) all solid ingredients, including cementitious materials and fine aggregate, were first mixed at a low speed for 3 minutes; 2) the mixing water was premixed with HRWR and was then mixed with the dry ingredients for 3 minutes; 3) after forming a uniform mortar mixture, the fiber was discharged and mixed for an additional 3 minutes at a low speed. It was lastly mixed at a medium speed for 1 minute. The fresh ECC was cast into the dogbone-shaped specimens (with dimensions shown in Fig. 4) and 100 mm (4 in.) cube specimens for uniaxial tension and compression tests, respectively. All specimens were cured for 28 days at room condition before testing.

Material testing

The ECC mechanical tests include unconfined compression (ASTM C109) and uniaxial tension (JSCE[19]). The compression test was conducted on the 100 mm (4 in.) ECC cubes at a loading rate of 0.5 MPa/s (72.5 psi/s). The tension test was conducted on the dogbone-shaped specimens at a displacement-controlled loading rate of 0.5 mm/min (0.02 in./min). A universal testing system was used. To measure the tensile strain, a pair of linear variable differential transducers (LVDT) was mounted on the specimen. The center 80 mm (3.14 in.) long section was chosen as the gauged area for tensile strain measurement. Besides the mechanical testing, an additional set of specimens was pre-strained to 2% in tension and subsequently underwent a self-healing test. After pre-straining, the crack width distribution was first measured on the specimen surface in the 80 mm (3.14 in.) center section using an optical microscope. The specimens were then exposed to a cyclic wet-dry environment, including 24-hour water immersion followed by 24-hour air drying. As an indicator of the self-healing process, the specimen's resonance frequency (RF) was measured up to seven wet-dry cycles. The RF recovery ratio was determined using Eq. (3)

$$R_{RF} = \frac{RF_{pre\text{-}cracked}}{RF_{non\text{-}cracked}} \times 100\% \quad (3)$$

where R_{RF} is the recovery ratio of resonance frequency led by self-healing; $RF_{pre\text{-}cracked}$ is the resonance frequency of the pre-cracked specimen; and $RF_{non\text{-}cracked}$ is the resonance frequency of the non-cracked specimen.

EXPERIMENTAL RESULTS AND DISCUSSION

CO_2 uptake in fly ash and steel slag

The results of raw materials carbonation suggest that an optimal range of water-to-solid ratio (*w*/*s*) for maximizing CO_2 uptake in fly ash and steel slag exists. As shown in Fig. 5 and 6, the optimal *w*/*s* seemingly lies close to 0.15 for steel slag and 0.15 to 0.20 for fly ash. Increasing or decreasing the water content was found to lower the CO_2 uptake for the same sample. As noted by Baciocchi et al.[20] and Huijgen et al.,[21] a liquid environment is necessary for initiating the solvation of Ca and Mg ions, which subsequently combine with the dissolved CO_3^{2-} ions. A high water content, on the other hand, tends to dilute the ionic concentration, thus slowing down the reaction kinetics. In these cases, a finer sample particle size, a higher temperature, and an elevated CO_2 partial pressure were found desirable to promote the reaction rate and actual CO_2 uptake, thus approaching the maximal CO_2 sequestration capacity. Nevertheless, when used as ingredients for ECC, the particle sizes of fly ash and steel slag are controlled by the composite micromechanical design. A further grinding process also involves uncertain energy penalty that partially offsets the net emission reduction. Likewise, heating and pressurization are not favorable for scaled implementation due to the additional process complexity and risk for industrial deployment and are thus not prioritized in this study. The effects of such processes

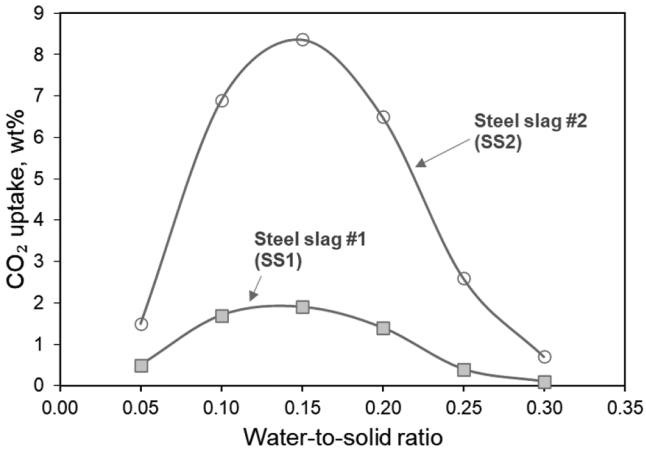

Fig. 5—Effect of w/s *on steel slag CO_2 uptake.*

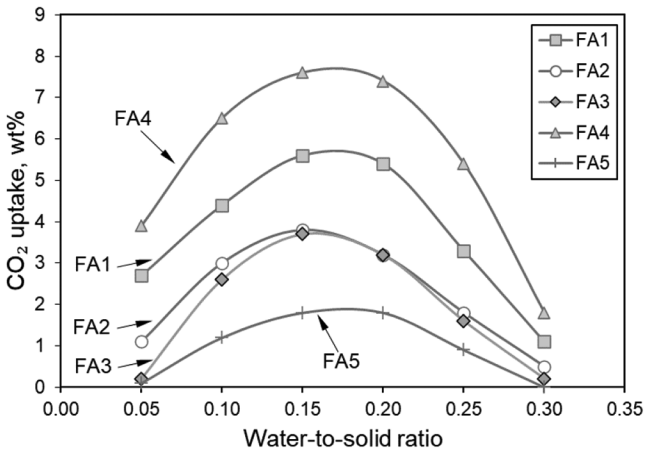

Fig. 6—Effect of w/s *on fly ash CO_2 uptake.*

as grinding, heating, and pressurization on ECC's technical properties and net CO_2 emissions are beyond the scope of this study and merit further investigation. Based on the results shown in Fig. 5 and 6, a *w/s* of 0.15 was chosen for fly ash and steel slag carbonation.

The evolution of CO_2 uptake regarding carbonation time suggests that 2-hour carbonation is sufficient to approach the maximal CO_2 uptake in the predetermined condition. Figures 7 and 8 show the CO_2 uptake measured after different carbonation durations, and it was found that 15-minute carbonation can attain more than 80% of the 2-hour CO_2 uptake for all samples. Steel slag and fly ash showed similar kinetics of CO_2 uptake, which appeared to decrease significantly over reaction time and level off after 1 hour. This trend is consistent with the findings of previous studies,[20] which attributed the declining reaction rate to the limited availability of Ca ions associated with the solubility of Ca-bearing phases in solid wastes. As suggested by Huijigen et al.,[21] Ca from portlandite and calcium silicates such as CSH is easily leachable and thus more reactive in the early reaction stage. Calcium silicates that are more difficult to dissolve tend to react more slowly. It was found that, without introducing additional heating or pressurization treatment, the samples used in the present study can be carbonated adequately within 2 hours of carbonation.

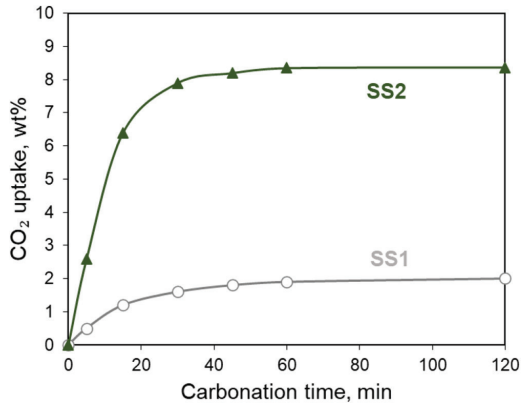

Fig. 7—Steel slag CO_2 uptake evolution in 2-hour carbonation.

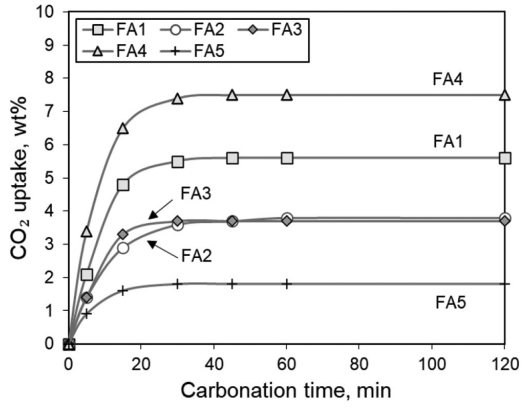

Fig. 8—Fly ash CO_2 uptake evolution in 2-hour carbonation.

The aforementioned experimental trials informed the carbonation condition adopted for ECC ingredients carbonation—that is, 0.15 *w/s* at room temperature and 1.5-bar (21.8 psi) pressure. The carbonation duration was chosen as 2 hours. Table 4 lists the optimal CO_2 uptake measured in the five sources of Class C fly ash, two sources of steel slag, and the control groups including Class F fly ash (FA0) and silica sand (SS0). Among all samples, FA4 and SS1 exhibited the highest CO_2 uptake, measuring 7.53% and 8.37%, respectively. The XRD patterns shown in Fig. 9 and 10 confirmed the evidence of calcite precipitation in the absence of portlandite in all carbonated samples. By contrast, the control groups FA0 and SS0 did not show measurable CO_2 uptake under the same carbonation condition.

Properties of ECC made with carbonated materials

The ECC specimens made with carbonated steel slag and fly ash exhibited the comparable mechanical properties relative to the regular ECC made with non-carbonated silica sand and fly ash. As shown in Table 5, at 3 days, the compressive strength appeared to be 13.6% higher for ECC-C than ECC-R. As the subsequent hydration proceeds, the difference in compressive strength was found to decrease and appeared to be statistically insignificant at 28 days—that is, 31.1 ± 1.0 MPa (4511 ± 145 psi) for ECC-R and 32.2 ± 1.2 MPa (4670 ± 174 psi) for ECC-C.

Figure 11 shows the uniaxial tensile stress-strain relationship at 28 days, where both groups exhibited distinct

strain-hardening characteristics and comparable tensile properties including first-cracking tensile strength, ultimate tensile strength, and tensile strain capacity. As shown in Table 5, the difference between the tensile properties of ECC-C and ECC-R was found to be less than 10% and was statistically insignificant considering the standard deviation. The tensile strain capacity of ECC-R was relatively low compared to those reported in previous studies, potentially due to the incorporation of high-CaO fly ash. As reported by Kan et al.,[22] increasing fly ash CaO content from 7.65 wt.% to 16.4 wt.% can decrease ECC tensile strain capacity from 3.81% to 2.49% at 28 days. In PC-fly ash blends, a high fly ash CaO content tends to increase the cementing ability, thus leading to a higher compressive strength compared to low-CaO fly ash.[22,23] The higher fly ash reactivity may also increase the matrix toughness J_{tip} in ECC, thus decreasing the composite strain-hardening potential.[8] Although Class F fly ash with a low CaO content is favorable for ECC, the diminishing supply of quality Class F necessitates the search for low-grade alternatives, and Class C fly ash represents a suitable feedstock.

Table 4—Maximal CO_2 uptake by ECC ingredients

Sample batch		CO_2 uptake, wt%
Fly ash	FA0 (control)	0.00
	FA1	5.57
	FA2	3.82
	FA3	3.74
	FA4	7.53
	FA5	1.85
Silica sand	SS0 (control)	0.00
Steel slag	SS1	8.37
	SS2	1.96

In addition to comparable mechanical properties, ECC-C and ECC-R showed comparable crack width control and self-healing behavior. As shown in Table 6, after pre-straining to 2% in tension, ECC-C and ECC-R had residual average crack widths of 38 μm (1.5 × 0.001 in.) and 42 μm (1.7 × 0.001 in.), respectively. Compared to ECC-R, ECC-C showed a slightly more saturated multiple cracking behavior, with a higher number of cracks and a lower average crack spacing. The two ECC groups also exhibited similar self-healing processes. As shown in Fig. 12, for both groups, the RF ratio recovered from 55 to 60% after pre-cracking to above 95% after seven wet-dry cycles. The RF recovery was rapid in the first one to three cycles and slowed down after the fourth cycle. As an indicator of the self-healing process, the RF evolution suggested that the incorporation of carbonated ingredients had a marginal impact on ECC's self-healing capability.

Estimated emission reduction

The net CO_2 emissions are estimated on a cradle-to-gate basis based on the ECC laboratory processing and are expressed in the unit of global warming potential (GWP, kg CO_{2eq}). The system boundary includes the typical A1 (raw material extraction), A2 (transport), and A3 (manufacturing) stages according to EN 15804/EN 15978. In the A1 stage, CO_2 emissions associated with the upstream production of all raw materials are considered, including the carbonation process. Table 7 lists A1 data inventory.[24-27] The non-carbonated steel slag is assumed as a waste stream with no incoming environmental burden, while CO_2 sequestration is counted as negative emissions based on the experimental data in the present study. As steel slag was sieved and reproportioned without grinding, no energy penalty was involved. In field practice, fly ash and steel slag are anticipated to be carbonated directly in the flue gas streams of coal power plants or steelmaking plants, and therefore the emissions for capturing and transporting CO_2 is excluded. Tables 8 and 9

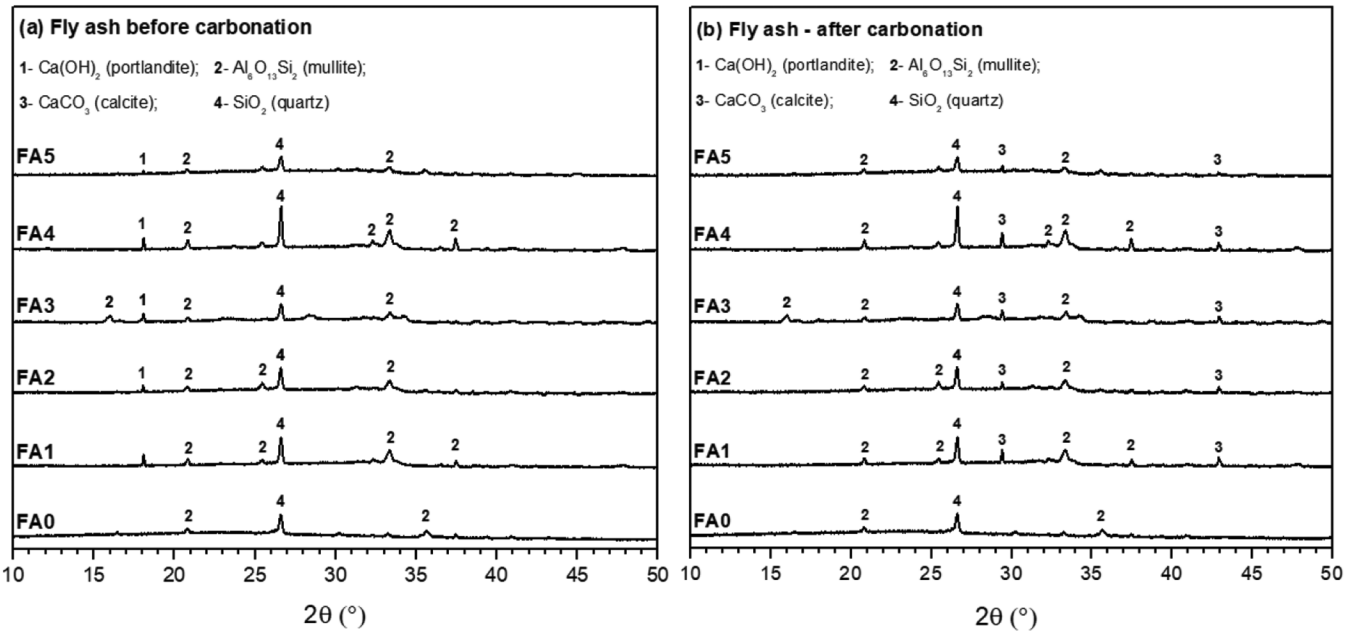

Fig. 9—XRD patterns of fly ash samples before and after carbonation.

Table 5—ECC mechanical properties

Mechanical properties	Age	ECC-C	ECC-R
Compressive strength, MPa (psi)	3 days	12.5 ± 0.5 (1813 ± 73)	14.2 ± 0.5 (2060 ± 73)
	7 days	27.3 ± 1.0 (3960 ± 145)	27.5 ± 0.4 (3989 ± 58)
	28 days	32.2 ± 1.2 (4670 ± 174)	31.1 ± 1.0 (4511 ± 145)
First cracking tensile strength, MPa (psi)	28 days	2.4 ± 0.2 (348 ± 29)	2.2 ± 0.1 (324 ± 15)
Ultimate tensile strength, MPa (psi)	28 days	3.6 ± 0.2 (524 ± 29)	3.6 ± 0.1 (524 ± 15)
Tensile strain capacity, %	28 days	2.9 ± 0.6	3.0 ± 0.3

Table 6—Residual crack width and crack spacing

Batch	Crack width, μm (× 0.001 in.)		Crack number	Average crack spacing, mm (in.)
	Average	Maximum		
ECC-R	42 (1.7)	61 (2.4)	33	2.4 (0.094)
ECC-C	38 (1.5)	52 (2.0)	39	2.1 (0.083)

Note: Residual cracks measured on ECC specimens pre-strained to 2%.

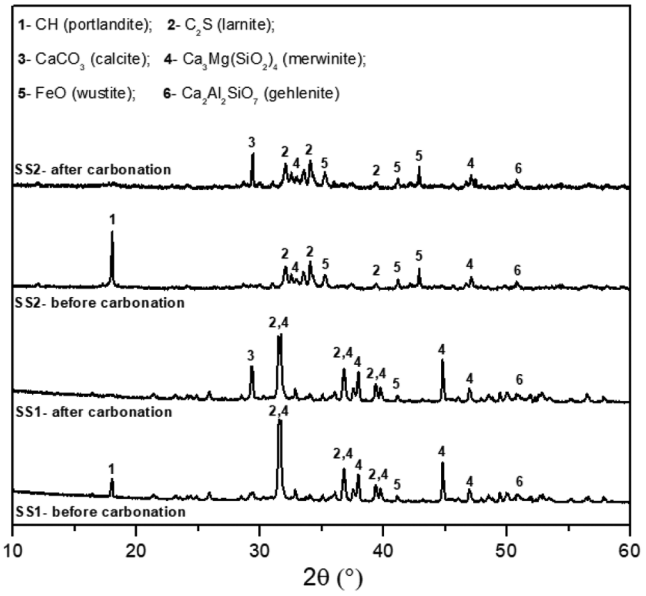

Fig. 10—XRD patterns of steel slag samples before and after carbonation.

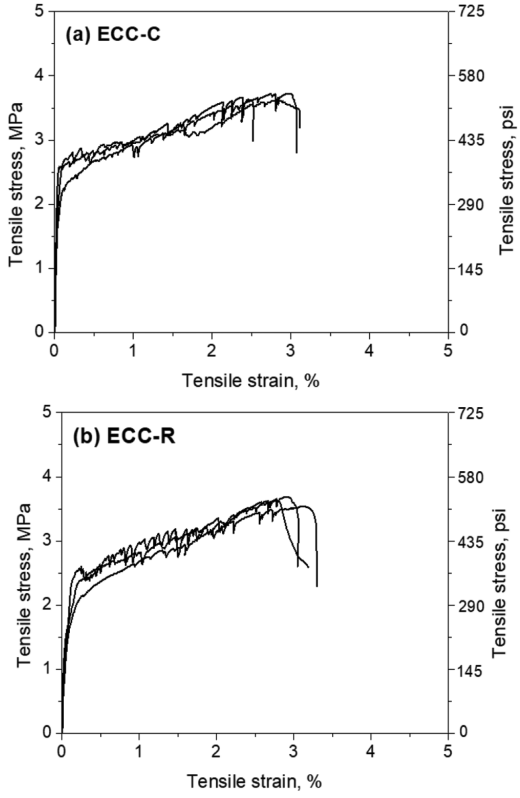

Fig. 11—ECC tensile curves at 28 days: (a) ECC-C; and (b) ECC-R.

list the data inventory for the A2 stage—that is, transport of raw materials to a concrete mixing plant. The transport mode and distance of most raw materials (except metakaolin[24] and steel slag) are collected on a national average basis in the U.S. context.[28] For the A3 stage, the energy input and associated emissions are assumed to be the same between ECC and regular concrete and are based on the NRMCA national average data shown in Table 10.[28] The emissions are calculated for 1 m^3 (1.308 yd^3) of ECC/concrete. As for comparison, an averaged mixture design of 27.6 MPa (4000 psi) concrete[28] is analyzed in parallel to the ECC-R and ECC-C groups.

The results of the estimated carbon emissions are graphically illustrated in Fig. 13 through 16. As shown in Fig. 13, the total A1-A3 emissions follow a distinctly descending order from regular concrete to ECC-R, then to ECC-C. Comparing ECC-R with regular concrete, it is found that the coupled use of limestone and metakaolin is conducive to the emission reduction while maintaining the same level of compressive strength. By incorporating the carbonated ingredients, ECC-C further decreases the carbon emissions to 236.08 kg-CO_{2eq}/m^3 (397.93 lb-CO_{2eq}/yd^3), 42.0% lower than that of the 27.6 MPa (4000 psi) concrete and 32.6% lower than that of ECC-R. This substantial reduction in the CO_2 footprint mainly stems from the A1 stage, where the emissions for 27.6 MPa (4000 psi) concrete, ECC-R, and ECC-C are found to be 397.51, 328.08, and 213.82 kg-CO_{2eq}/m^3 (670.02, 553.00, and 360.41 lb-CO_{2eq}/yd^3), respectively. The combined use of low-carbon binder (PC + metakaolin + limestone) and CO_2-sequestered ingredients collectively curbed the A1 emissions by nearly half and demonstrated a potential

path to carbon neutrality by further lowering the clinker content and enhancing CO_2 uptake in the raw ingredients.

The A1 and A2 emissions are broken down into the individual impact of each ingredient for ECC-R and ECC-C as shown in Fig. 14 and 15. For both mixtures, PC is found to be the largest contributor to A1 emissions, followed by polymeric fiber and metakaolin. By replacing silica sand with carbonated steel slag, ECC-C can avoid 16.92 kg-CO_{2eq}/m^3 (28.52 lb-CO_{2eq}/yd^3) emissions associated with the aggregate production and 41.47 kg-CO_{2eq}/m^3 (69.90 lb-CO_{2eq}/yd^3) emissions by sequestering CO_2 in steel slag. Incorporating carbonated fly ash further offsets 36.07 kg-CO_{2eq}/m^3 (60.80 lb-CO_{2eq}/yd^3) emissions. These results suggest that reducing PC content and increasing the total CO_2 uptake in fly ash and steel slag are the most effective strategy for lowering A1 emissions in ECC-C.

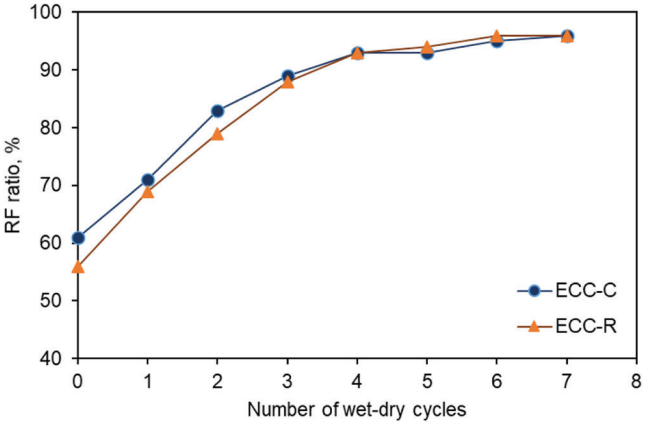

Fig. 12—Partial recovery of resonance frequency of pre-cracked ECC during self-healing.

The A2 GWP appear to be comparable between ECC-C and ECC-R. As shown in Fig. 15, the transport-associated emissions remain unchanged for PC, metakaolin, limestone, fly ash, and polymeric fiber due to the same material use and the same transport data inventories between ECC-C and ECC-R. As steel slag is not a commonly used standard feedstock for concrete, its transport distance was collected from a local survey based on the actual locations of the steelmaking plant and concrete mixing plant. This distance and transport mode are not representative of the national average. Nevertheless, it is suggestive in Fig. 15 that the contribution of steel slag transport is moderate compared to those of metakaolin and fly ash. It is noteworthy that the transport of metakaolin is significant due to the long trucking distance used in this study, which warrants further investigation to facilitate a more precise understanding of the emissions impact of transporting metakaolin in the North American region.

Table 7—Life-cycle inventory of raw materials processing and extraction (A1 stage)

Materials	GWP kg/kg $CO_{2\text{-eq}}$	Data source
Cement	0.922	PCA[25]
Metakaolin	0.253	Nguyen et al.[24]
Limestone	0.007	Miller et al.[27]
Fly ash, non-carbonated	0.027	Miller et al.[27]
Fly ash, carbonated	–0.0449	Experimental data in this study and Miller et al.[27]
Steel slag, non-carbonated	—	None, no incoming burden
Steel slag, carbonated	–0.0771	Experimental data in this study
Silica sand, natural	0.04	GaBi 6.0 database
Water	0.000658	Eco-invent database
Polymeric fiber	2.3336	Eco-invent database
HRWRA	1.88	EFCA[26]

Note: Steel slag is considered as industrial by-product, and its environmental impact before carbonation is not included in this study.

Table 8—Average transport distance from extraction location to ready mix plant (A2 stage)

Materials	Truck, km (mile)	Rail, km (mile)	Ocean, km (mile)	Barge, km (mile)
Cement	117.6 (73.1)	71.0 (44.1)	113.6 (70.6)	56.0 (34.8)
Metakaolin	2723.0 (1692)	0.0 (0.0)	0.0 (0.0)	0.0 (0.0)
Limestone, mineral fillers	5.3 (3.3)	1.4 (0.9)	0.0 (0.0)	0.0 (0.0)
Fly ash, processed	47.0 (29.2)	41.5 (25.8)	0.0 (0.0)	4.0 (2.5)
Steel slag	46.7 (29.0)	0.0 (0.0)	0.0 (0.0)	0.0 (0.0)
Natural sand	54.1 (33.6)	1.1 (0.7)	10.3 (6.4)	7.6 (4.7)
Polymeric fiber	73.1 (45.4)	0.0 (0.0)	0.0 (0.0)	0.0 (0.0)
HRWRA	259.4 (161.2)	0.0 (0.0)	0.0 (0.0)	0.0 (0.0)

Note: Metakaolin data is from Nguyen et al.[24] based on field survey and is assumed to be transported by truck. Steel slag data is from local survey conducted in Southeast Michigan region. Other data are sourced from NRMCA national average.

Table 9—GWP of transport mode (A2 stage)

Transport mode	GWP, $CO_{2\text{-eq}}$	
	kg/(km·tonne)	lb/(mile·ton)
Truck	0.052	0.167
Rail	0.028	0.090
Ocean/Barge	0.016	0.051

Note: Data is from Nguyen et al.[24] Data for ocean is assumed to be same as for barge.

Table 10—Energy use for ECC/concrete mixing (A3 stage)

Energy source	Energy use	
Electricity	kWh/m^3	kWh/yd^3
	4.88	3.73
Natural gas	L/m^3	ft^3/yd^3
	296.67	8.01
Fuel oil (other than diesel)	L/m^3	gal./yd^3
	0.04	0.01
Diesel	L/m^3	gal./yd^3
	1.93	0.39
LPG (liquified propane gas)	L/m^3	gal./yd^3
	0.08	0.01

Note: Data sourced from NRMCA national average. Associated emission impact is calculated based on U.S. LCI database.

Figure 16 shows the contour graph of ECC's carbon footprint through the A1 to A3 stages, plotted against the CO_2 uptake in steel slag and fly ash. The two shaded areas represent the GWP of ECC-C incorporating various steel slag and fly ash samples examined in this study (SS1 and 2 and FA1 to 5) and the prospective ECC-C with negative emissions. Based on the ECC-C mixture design, carbon negativity can be plausibly achieved by increasing the steel slag and fly ash CO_2 uptake to above ~20% simultaneously, assuming no carbon penalty was involved in the carbonation process. This level of CO_2 uptake is stoichiometrically possible for both steel slag samples and most fly ash samples shown in Table 1 but is expected to be associated with significant energy barriers to activate the Ca-bearing phases and dissolve sufficient Ca ions. Emerging clean energy—for example, solar power—may be used to facilitate a favorable environment of temperature and CO_2 partial pressure, and the associated impact on life-cycle emissions should be further investigated.

Considerations for field practice

The present study is preliminary and aims to prove the concept at the laboratory scale. In transferring the process to the field, a significant effort of industrial research and development is needed. It is recommended to deploy the carbonation process in the vicinity of CO_2 point sources—for example, carbonating fly ash at the same coal power plant where the fly ash is generated and carbonating steel slag at the same steelmaking plant. In these scenarios, CO_2 in the flue gas may be used directly for the carbonation process, and the residual waste heat carried by the flue gas can be

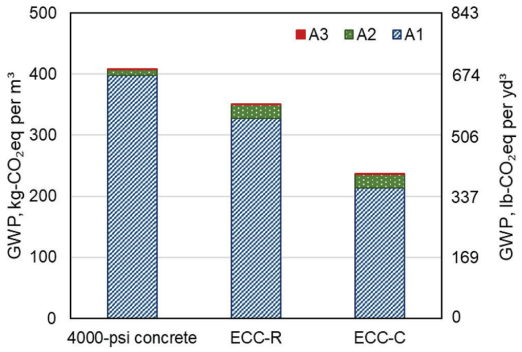

Fig. 13—GWP from A1 through A3 stages for 27.6 MPa (4000 psi) concrete, ECC-R, and ECC-C.

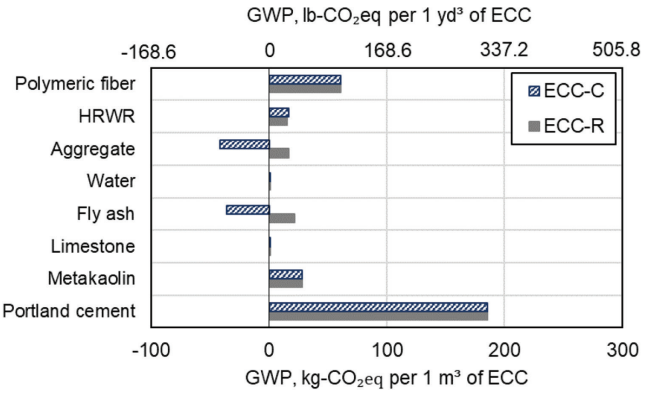

Fig. 14—A1 stage GWP distribution of ECC-R and ECC-C.

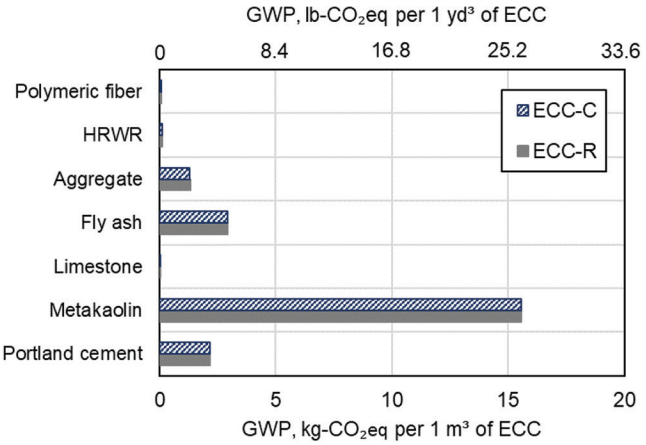

Fig. 15—A2 stage GWP distribution of ECC-R and ECC-C.

potentially recycled and used to maintain a favorable reaction temperature. As typical by-products, fly ash and steel slag extraction time and location would involve a significant variability in the material composition and thus the actual CO_2 uptake. Hence, adapting the carbonation process to local ingredients may be critical to ensure consistent climate benefits.

Apart from carbonation, grinding steel slag may involve a large energy penalty and should be further investigated. At the lab scale, steel slag samples were sieved for fine particles and minimal energy was consumed for sieving. Nevertheless, raw steel slags usually have a particle size comparable to coarse aggregate, and a grinding process seems inevitable to attain a high utilization efficiency. Due to the relatively

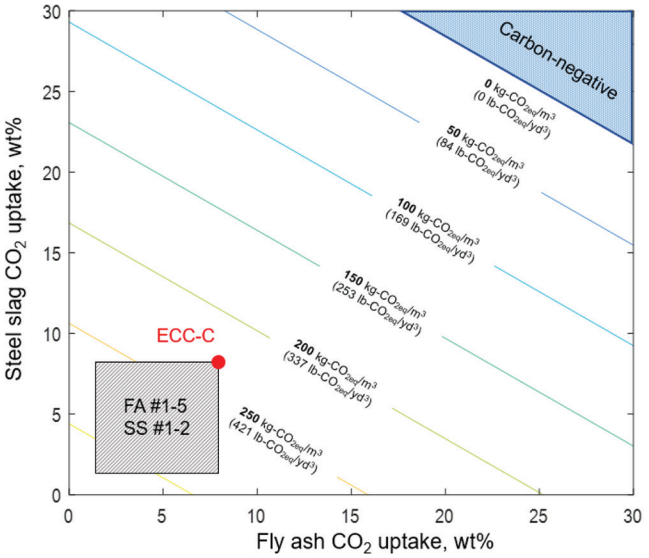

Fig. 16—Effect of fly ash and steel slag CO_2 uptake on A1 through A3 (cradle-to-gate) emissions of ECC-C at 27.6 MPa (4000 psi) strength level.

high specific gravity and hardness of steel slag, the grinding process may involve considerable energy input and hardware investment, which should be further understood before implementation.

SUMMARY AND CONCLUSIONS

This study demonstrates the concept of sequestering CO_2 in durable engineered cementitious composites (ECC) for cast-in-place construction. By incorporating carbonated steel slag and high-CaO fly ash, ECC can achieve a 42% reduction in the cradle-to-gate carbon emissions relative to regular concrete at the same compressive strength level. The composite mechanical properties show no statistically significant differences between the ECC groups made with and without CO_2-sequestered ingredients. At 28 days, CO_2-sequestered ECC attains a compressive strength of 32.2 MPa (4670 psi), an ultimate tensile strength of 3.6 MPa (524 psi), and a tensile strain capacity of 2.9%. The self-healing capability is also maintained as indicated by the partial recovery of resonance frequency, suggesting the possibility of decarbonizing the embodied and use-phase emissions by deploying ECC in the built environment.

Among the A1 through A3 stages in the typical lifecycle framework, the material extraction (A1) stage contributes 90.6% of total emissions for CO_2-sequestered ECC, with portland cement (PC) accounting for 185.32 kg CO_{2eq} per 1 m^3 of ECC (312.37 lb-CO_{2eq}/yd^3). This indicates that lowering cement emissions or reducing cement use remains to be a key step for further decarbonizing ECC. With the portland cement (PC) binder system, at least a 20 wt% CO_2 uptake in both fly ash and steel slag is necessary to offset the total emissions and achieve carbon neutrality.

Further investigations may explore affordable and low-carbon approaches for maximizing CO_2 uptake in fly ash and steel slag. As industrial by-products, the associated large variability in the material composition should be recognized, and a more refined life-cycle assessment extending beyond the A3 stage is needed. Additionally, further experimental research may address the scalability and durability of the CO_2-sequestered ECC through outdoor testing and investigate its practical applications and end-of-life treatment.

AUTHOR BIOS

Duo Zhang *is a Professor at Wuhan University, Wuhan, China, and previously an Assistant Research Scientist at the University of Michigan and the Center for Low-Carbon Built Environment, Ann Arbor, MI. He received his PhD in civil engineering from McGill University, Montreal, QC, Canada, in 2016. His research interests include concrete sustainability, CO_2 sequestration, and fiber-reinforced cementitious composites.*

Victor C. Li, *FACI, is the James R. Rice Distinguished University Professor of Engineering at the University of Michigan and the founding Director of the Center for Low-Carbon Built Environment. His research interests include the micromechanics and design of ultra-ductile and green cementitious composites, their application to innovative and sustainable infrastructure systems, and integration of materials and structural design.*

ACKNOWLEDGMENTS

The financial supports from the University of Michigan's College of Engineering BlueSky Project and the Center for Low-Carbon Built Environment are gratefully acknowledged.

REFERENCES

1. Barcelo, L.; Kline, J.; Walenta, G.; and Gartner, E., "Cement and Carbon Emissions," *Materials and Structures*, V. 47, No. 6, 2014, pp. 1055-1065. doi: 10.1617/s11527-013-0114-5

2. Zhang, D.; Ghouleh, Z.; Shao, Y., "Review on Carbonation Curing of Cement-Based Materials," *Journal of CO2 Utilization*, V. 21, 2017, pp. 119-131.

3. Berger, R.; Young, J.; and Leung, K., "Acceleration of Hydration of Calcium Silicates by Carbon Dioxide Treatment," *Nature. Physical Science (London)*, V. 240, No. 97, 1972, pp. 16-18. doi: 10.1038/physci240016a0

4. Vandeperre, L., and Al-Tabbaa, A., "Accelerated Carbonation of Reactive MgO Cements," *Advances in Cement Research*, V. 19, No. 2, 2007, pp. 67-79. doi: 10.1680/adcr.2007.19.2.67

5. Cizer, Ö.; Van Balen, K.; Elsen, J.; and Van Gemert, D., "Real-Time Investigation of Reaction Rate and Mineral Phase Modifications of Lime Carbonation," *Construction and Building Materials*, V. 35, 2012, pp. 741-751. doi: 10.1016/j.conbuildmat.2012.04.036

6. Monkman, S., and MacDonald, M., "On Carbon Dioxide Utilization as a Means to Improve the Sustainability of Ready-Mixed Concrete," *Journal of Cleaner Production*, V. 167, 2017, pp. 365-375. doi: 10.1016/j.jclepro.2017.08.194

7. Li, V. C., "On Engineered Cementitious Composites (ECC). A Review of the Material and Its Applications," *Journal of Advanced Concrete Technology*, V. 1, No. 1, 2003, pp. 215-230. doi: 10.3151/jact.1.215

8. Li, V. C., *Engineered Cementitious Composites (ECC): Bendable Concrete for Sustainable and Resilient Infrastructure*, Springer, New York, 2019.

9. Li, V. C., "Engineered Cementitious Composites (ECC)—Tailored Composites through Micromechanical Modeling," *Fiber Reinforced Concrete Present and Future*, N. Banthia, A. Bentur, and A. A. Mufti, eds., Canadian Society for Civil Engineering, Montreal, QC, Canada, 1997, pp. 64-97.

10. Yang, E. H., and Li, V. C., "A Micromechanical Model for Fiber Cement Optimization and Component Tailoring," 10th International Inorganic-Bonded Fiber Composites Conference, Sao Paulo, Brazil, 2006.

11. Li, M., and Li, V. C., "Cracking and Healing of Engineered Cementitious Composites under Chloride Environment," *ACI Materials Journal*, V. 108, No. 3, May-June 2011, pp. 333-340.

12. Lepech, M. D., and Li, V. C., "Water Permeability of Engineered Cementitious Composites," *Cement and Concrete Composites*, V. 31, No. 10, 2009, pp. 744-753. doi: 10.1016/j.cemconcomp.2009.07.002

13. Li, V. C., and Yang, E. H., "Self Healing in Concrete Materials," *Self-Healing Materials*, Springer, Dordrecht, the Netherlands, 2007, pp. 161-193.

14. Li, V. C., and Herbert, E., "Robust Self-Healing Concrete for Sustainable Infrastructure," *Journal of Advanced Concrete Technology*, V. 10, No. 6, 2012, pp. 207-218. doi: 10.3151/jact.10.207

15. Keoleian, G. A.; Kendall, A.; Dettling, J. E.; Smith, V. M.; Chandler, R. F.; Lepech, M. D.; and Li, V. C., "Life Cycle Modeling of Concrete Bridge Design: Comparison of Engineered Cementitious Composite Link Slabs and Conventional Steel Expansion Joints," *Journal of*

Infrastructure Systems, ASCE, V. 11, No. 1, 2005, pp. 51-60. doi: 10.1061/(ASCE)1076-0342(2005)11:1(51)

16. Zhang, D.; Ellis, B. R.; Jaworska, B.; Hu, W.-H.; and Li, V. C., "Carbonation Curing for Precast Engineered Cementitious Composites," *Construction and Building Materials*, V. 313, 2021, p. 125502. doi: 10.1016/j.conbuildmat.2021.125502

17. Wu, H.-L.; Zhang, D.; Ellis, B. R.; and Li, V. C., "Development of Reactive MgO-Based Engineered Cementitious Composite (ECC) through Accelerated Carbonation Curing," *Construction and Building Materials*, V. 191, 2018, pp. 23-31. doi: 10.1016/j.conbuildmat.2018.09.196

18. Scrivener, K.; Martirena, F.; Bishnoi, S.; and Maity, S., "Calcined Clay Limestone Cements (LC3)," *Cement and Concrete Research*, V. 114, 2018, pp. 49-56. doi: 10.1016/j.cemconres.2017.08.017

19. JSCE, *Recommendations for Design and Construction of High Performance Fiber Reinforced Cement Composites with Multiple Fine Cracks (HPFRCC)*, Tokyo, Japan, 2008.

20. Baciocchi, R.; Costa, G.; Polettini, A.; and Pomi, R., "Influence of Particle Size on the Carbonation of Stainless Steel Slag for CO_2 Storage," *Energy Procedia*, V. 1, No. 1, 2009, pp. 4859-4866. doi: 10.1016/j.egypro.2009.02.314

21. Huijgen, W. J.; Witkamp, G.-J.; and Comans, R. N., "Mineral CO_2 Sequestration by Steel Slag Carbonation," *Environmental Science & Technology*, V. 39, No. 24, 2005, pp. 9676-9682. doi: 10.1021/es050795f

22. Kan, L.; Shi, R.; and Zhu, J., "Effect of Fineness and Calcium Content of Fly Ash on the Mechanical Properties of Engineered Cementitious Composites (ECC)," *Construction and Building Materials*, V. 209, 2019, pp. 476-484. doi: 10.1016/j.conbuildmat.2019.03.129

23. Mehta, P. K., "Influence of Fly Ash Characteristics on the Strength of Portland-Fly Ash Mixtures," *Cement and Concrete Research*, V. 15, No. 4, 1985, pp. 669-674. doi: 10.1016/0008-8846(85)90067-5

24. Nguyen, L.; Moseson, A. J.; Farnam, Y.; and Spatari, S., "Effects of Composition and Transportation Logistics on Environmental, Energy and Cost Metrics for the Production of Alternative Cementitious Binders," *Journal of Cleaner Production*, V. 185, 2018, pp. 628-645. doi: 10.1016/j.jclepro.2018.02.247

25. PCA, "Environmental Product Declaration—Portland Cement," Portland Cement Association, Skokie, IL, 2021.

26. EFCA, "Environmental Product Declaration—Concrete Admixtures – Plasticisers and Superplasticisers," European Federation of Concrete Admixtures Associations Ltd., 2015.

27. Miller, S. A.; John, V. M.; Pacca, S. A.; and Horvath, A., "Carbon Dioxide Reduction Potential in the Global Cement Industry by 2050," *Cement and Concrete Research*, V. 114, 2018, pp. 115-124. doi: 10.1016/j.cemconres.2017.08.026

28. Bushi, L., and Finlayson, G., "NRMCA Member National and Regional Life Cycle Assessment Benchmark (Industry Average) Report," National Ready Mixed Concrete Association, Alexandria, VA, Oct. 2014.